JOURNAL OF APPLIED ELECTROCHEMISTRY 20 (1990) 728–736

The effects of antimony and glue on zinc electrowinning from Kidd Creek electrolyte

D. J. MACKINNON, R. M. MORRISON

Metallurgical Chemistry Section, Mineral Sciences Laboratories, CANMET, Energy, Mines and Resources Canada, 555 Booth Street, Ottawa, Ontario, Canada K1A 0G1

J. E. MOULAND, P. E. WARREN

Falconbridge Ltd., Kidd Creek Division, P.O. Box 2002, Timmins, Ontario, Canada P4N 7K1

Received 20 October 1989

The individual and combined effects of antimony and glue on zinc deposition current efficiency and polarization and on the morphology and orientation of 6 h zinc deposits electrowon at 500 A m^{-2} and 38° C from Kidd Creek zinc electrolyte were determined. Glue increased zinc deposition polarization, reduced the deposit grain size, changed the preferred deposit orientation from basal to intermediate, but decreased the current efficiency. At concentrations above 0.02 mg l^{-1}, antimony had a strong depolarizing effect on zinc deposition resulting in a basal deposit orientation and very low current efficiency. Certain combinations of antimony and glue, however, optimized zinc deposition current efficiency and consistently gave an intermediate ⟨114⟩⟨112⟩⟨103⟩⟨102⟩⟨101⟩ preferred deposit orientation. A correlation was observed between the current efficiency (CE) and the nucleation overpotential (NOP) for zinc deposition such that the CE was a maximum when the NOP of the initial cell electrolyte was 120–130 mV and when the NOP of the final cell electrolyte was 100–110 mV.

1. Introduction

Organic reagents such as animal glue are often added to zinc electrolyte at low concentrations (< 30 mg l^{-1}) to produce a smooth, compact zinc deposit. In spite of its beneficial levelling effect on the zinc deposit, increasing additions of animal glue to purified zinc electrolyte usually result in a decrease in the current efficiency (CE) for zinc deposition [1, 2]. Glue, however, also interacts in a beneficial way with certain impurities or additives in the electrolyte; for example, antimony, to optimize zinc deposition CE and modify the zinc deposit morphology and preferred orientation [1–6].

Antimony (at concentrations > 0.02 mg l^{-1}) has long been recognized as one of the most detrimental impurities with respect to zinc deposition CE [7–10], and its effects have most recently been studied by Ault and Frazer [11]. In spite of its detrimental effect on CE, a small concentration of antimony is usually added to the zinc electrolyte because it is thought to reduce zinc deposit adherence to the aluminum cathode blank and because of its beneficial interaction with glue.

In addition to optimizing CE and modifying the zinc deposit morphology, glue and antimony also have a significant effect on the zinc deposition overpotential [3, 12]. The addition of glue to the electrolyte increases the overpotential; that is, it polarizes zinc deposition whereas increasing concentrations of antimony decrease the overpotential. Balanced additions of glue and antimony produce a zinc deposition overpotential (nucleation overpotential, NOP) that results in an optimum value for the CE [13].

In the Kidd Creek zinc tankhouse, current operating practice includes the addition of antimony and sodium silicate to control the growth of the zinc deposit, of Dowfroth, a frothing agent, to form a layer of foam on the surface of the electrolyte to minimize acid mist formation and of $SrCO_3$ to control the level of lead in the zinc deposit. Dowfroth, however, in addition to controlling acid mist, also acts as a strong polarizer and thus affects zinc deposition CE and zinc deposit morphology. Because of its strong polarizing effect, which is counteracted to some extent by the antimony added to the electrolyte, the Dowfroth concentrations must be carefully controlled to avoid detrimental effects on the CE and deposit quality. Thus, the use of other foaming agents that do not strongly affect zinc deposition polarization is being considered. The use of non-polarizing foaming agents would obviate the close control necessary with Dowfroth but probably would require the presence of a polarizing additive such as animal glue to control the zinc deposit growth. As mentioned above, animal glue is a common addition agent in most zinc plants but is not presently added to the Kidd Creek electrolyte.

Thus, the present study was undertaken to assess the effects of glue, antimony, and glue + antimony on the CE and NOP for zinc deposition and on the morphology and orientation of zinc deposits electrowon from Kidd Creek zinc electrolyte

0021-891X/90 $03.00 + .12

2. Experimental details

2.1. *Electrolysis cell*

The electrolysis cells were constructed from 5 mm thick polycarbonate and had the approximate outside dimensions: 8.8 × 8.8 × 10.7 cm. A tight fitting cover (5 mm polycarbonate) was modified with holes to accommodate a central aluminium cathode, two anodes spaced ~6.3 cm centre to centre, feed and spent electrolyte tubing and a thermometer. The aluminium cathodes (supplied by Kidd Creek) were masked with electroplating tape to give a 2 in^2 (12.9 × 10^{-4} m^2) surface area. The cell held approximately 400 ml of electrolyte at 2/3 volume. For the 6 h electrolysis tests, Pt anodes were used to avoid lead contamination of the zinc deposits [14].

2.2. *Electrolyte composition*

Both feed and cell electrolytes were prepared from Kidd Creek purified neutral and cold spent solutions. The analyses are presented in Table 1. The electrolytes were prepared by diluting the as-received purified neutral solution with distilled water and reagent grade H_2SO_4. Some tests were also performed using the as-received cold spent solution as the cell electrolyte. The feed electrolyte contained ~100 $g l^{-1}$ Zn and ~130 $g l^{-1}$ H_2SO_4. The cell electrolytes contained 55 $g l^{-1}$ Zn and 200 $g l^{-1}$ H_2SO_4. The rate of addition of feed electrolyte to the cell was adjusted so that the cell zinc/acid concentration remained constant throughout the electrolysis.

The various additions (pearl glue and potassium antimony tartrate) were also supplied by Kidd Creek. These agents were added to both the feed and cell electrolytes at the desired concentrations as aliquots from stock solutions containing 1000 $mg l^{-1}$ glue and 30 $mg l^{-1}$ Sb.

Table 1. Analyses of neutral and cold spent solutions received from Kidd Creek

Analyte		*Neutral solution*	*Cold spent solution*
Mg	($g l^{-1}$)	2.3– 2.5	2.5– 2.8
Mn		9.7– 10.4	9.5– 10.5
Na		2.8– 3.0	2.7– 2.9
S		100.7–107.9	105.9–116.9
Zn		186.5–200.6	57.9– 64.0
H_2SO_4		–	196.0–208.0
Ag	($mg l^{-1}$)	1	1
Al		16– 20	28
As		<0.01	0.03
Sb		<0.01	<0.01
Se		<0.05	<0.05
Sn		<0.2	<0.2
Ba		0.6	1
Ca		305–350	309–313
Cd		0.6	<0.1
Co		0.2	0.3
Cr		<0.1	<0.1
Cu		0.1– 0.3	0.1
Fe		16– 20	15
Ga		<1	<1
In		<1	<1
Ni		<1	<1
Pb		1	1
Si		225–240	88– 94

2.3. *Experimental procedure*

The 6 h electrowinning tests were performed four at a time using cells immersed in a temperature controlled water bath. Feed and spent electrolytes were pumped into and out of the cells by an eight-channel peristaltic pump. The flow rate was set to a selected value and the composition of the feed was adjusted to maintain zinc and acid balances during electrolysis. The electrolytes were analyzed for zinc by atomic absorption spectrophotometry and for free H_2SO_4 by a 1,2-diaminocyclohexanetetraacetic acid (DCTA) modified base titration [15].

The water bath was controlled at 38° C and current was supplied at a constant 500 A m^{-2} current density to the cells by a regulated DC power supply.

At the end of the electrolysis period, the cathodes were pulled from the cells and the zinc deposits were rinsed with water, stripped, dried and weighed. The current efficiency was calculated from the weight of the zinc deposited and the charge passed. A portion of the final cell electrolyte was analyzed for Zn and free H_2SO_4, and the remainder was used to determine the polarization characteristics using cyclic voltammetry.

2.4. *Deposit examination*

Sections of the deposits were examined by X-ray diffraction (XRD) to determine their preferred orientation relative to the ASTM standard for zinc powder and by scanning electron microscopy (SEM) with a secondary electron detector (SED) to determine the deposit morphology.

2.5. *Polarization studies*

Cyclic voltammetry (CV) experiments were conducted to determine the polarization characteristics of zinc deposition for both the initial and final cell electrolytes for all the tests. The CV tests were executed in duplicate using 150 ml of electrolyte at room temperature. An aluminium disc cathode (2.8 cm^2), a Pt foil anode and a mercury/mercurous sulphate reference electrode (MSE) were used. The potential was cycled between −1.1 and −1.7 V with respect to MSE at a rate of 4 mV s^{-1} using a potentiostat driven by a voltage scan generator. The voltammograms were recorded as i against E plots using an X–Y recorder.

3. Results and discussion

3.1. *Glue effect*

The effect of glue additions, 0–60 $mg l^{-1}$, on the CE for 6 h zinc deposits electrowon at 500 A m^{-2} and 38° C is summarized in Table 2 and a plot of CE against glue concentration is shown in Fig. 1. These results indicate that the CE decreases with increasing

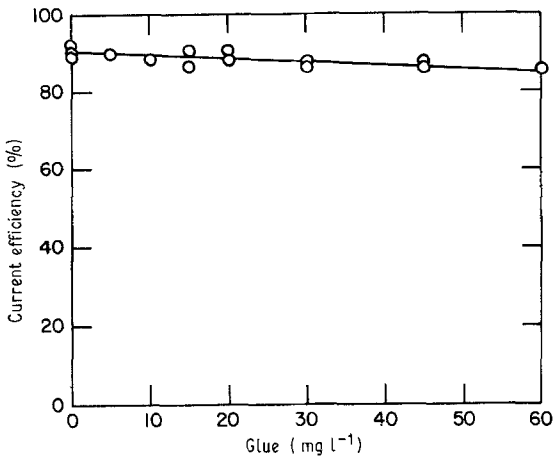

Fig. 1. Plot of current eficiency against glue concentration for 6 h zinc deposits electrowon at 500 A m^{-2} and 38° C.

glue addition; *viz*, from 91% at 0 mg l^{-1} glue to 85.9% at 60 mg l^{-1} glue. The incremental decrease in CE is 0.09% for each mg l^{-1} of added glue. Similar decreases in CE were reported by Robinson and O'Keefe [1] for glue additions to Cominco electrolyte.

The morphology of the 6 h zinc deposits electrowon from electrolyte containing various glue concentrations is shown in a series of SEM photographs, Fig. 2, and the deposit orientation results are summarized in Table 2.

In the absence of glue the zinc deposit consisted of closely packed nodules of varying grain size, Fig. 2a. Higher magnification indicated that these nodules consist of hexagonal zinc platelets aligned at low angles ($< 30°$) to the Al cathode, Fig. 2b. This results in a ⟨002⟩, ⟨103⟩ preferred deposit orientation, Table 2.

At 30 mg l^{-1} glue, the zinc deposit consists of closely packed nodules of reduced grain size compared to the glue-free case, *cf.* Figs 2a and 2c. In this case, the hexagonal zinc platelets, Fig. 2d, are aligned at $> 30°$ angles to the Al cathode, resulting in a ⟨114⟩, ⟨103⟩, ⟨112⟩, ⟨102⟩, ⟨101⟩ preferred orientation, Table 2. At 45 mg l^{-1} glue, a substantial grain refinement occurs although a few larger nodules are growing out of relief on the surface, Fig. 2e. As indicated in Fig. 2f, the hexagonal zinc platelets are now aligned at 30–60° angles to the Al cathode resulting in a ⟨112⟩, ⟨101⟩, ⟨114⟩ preferred orientation, Table 2. Thus, increasing glue additions to the electrolyte result in a more compact, grain refined zinc deposit with zinc platelets aligned at intermediate angles to the Al cathode. These results are generally in agreement with those obtained by Robinson and O'Keefe [1] who found that glue additions to Cominco electrolyte reduced the deposit grain size and at high concentrations (50 mg l^{-1}) caused the rotation of the platelet angle relative to the Al cathode from about 45° to 90° so that only the ⟨110⟩ type orientation was present.

The above results suggest that glue additions to zinc electrolyte increase zinc deposition polarization. The polarization was measured using cyclic voltammetry and a typical CV for addition-free electrolyte is shown in Fig. 3a. A scan is initiated at point A, −1.1 V with respect to MSE at a scan rate of 4 mV s^{-1}. An appreciable current begins to flow at point B (zinc decomposition potential) and the scan is reversed at point C; that is when the current is approximately 30 mA. At point D, the so-called crossover potential, the current is zero. After crossing point D, the current becomes anodic and zinc dissolves from the cathode; the anodic current reaches a maximum at point E and upon return to point A, zinc dissolution is complete.

The region B–D is termed nucleation overpotential (NOP) and it is the difference between the crossover potential D and the point B at which zinc begins to deposit. In the present work the point B was arbitrarily chosen to be the value of the potential when a current of 2.5 mA was reached in the forward scan.

The addition of glue to the electrolyte resulted in a significant change in the CV, most notably in the B–D portion (NOP region) of the curve, Fig. 3b. The NOP values for initial and final electrolytes were obtained for glue additions from 0 to 60 mg l^{-1}. These values are listed in Table 2 and shown as plots of NOP against glue concentration in Fig. 4. These data indi-

Table 2. The effect of glue on the current efficiency, orientation and nucleation overpotential (NOP) for 6 h zinc deposits electrowon at 500 A m^{-2} and 38° C

Glue (*mg l^{-1}*)	*CE* (%)	*Orientation**	*NOP (mV against MSE)*	
			Initial	*Final*
0	91.0	002, 103	140	125
5	90.1	002, 103, 101	130	140
10	88.8	103, 112, 114, 102	155	140
15	86.8	114, 103, 112, 102	157	155
15	91.5	103, 101	150	115
20	88.3	103, 114, 112, 102	155	145
20	91.2	–	145	120
30	86.8	103, 112, 114, 102	165	155
30	87.2	114, 103, 112, 102, 101	157	115
45	86.4	112, 103, 114, 102	170	143
45	87.8	112, 101, 114	173	150
60	85.9	114, 112, 103, 201, 101	175	117

* Relative to ASTM Standard for zinc powder.

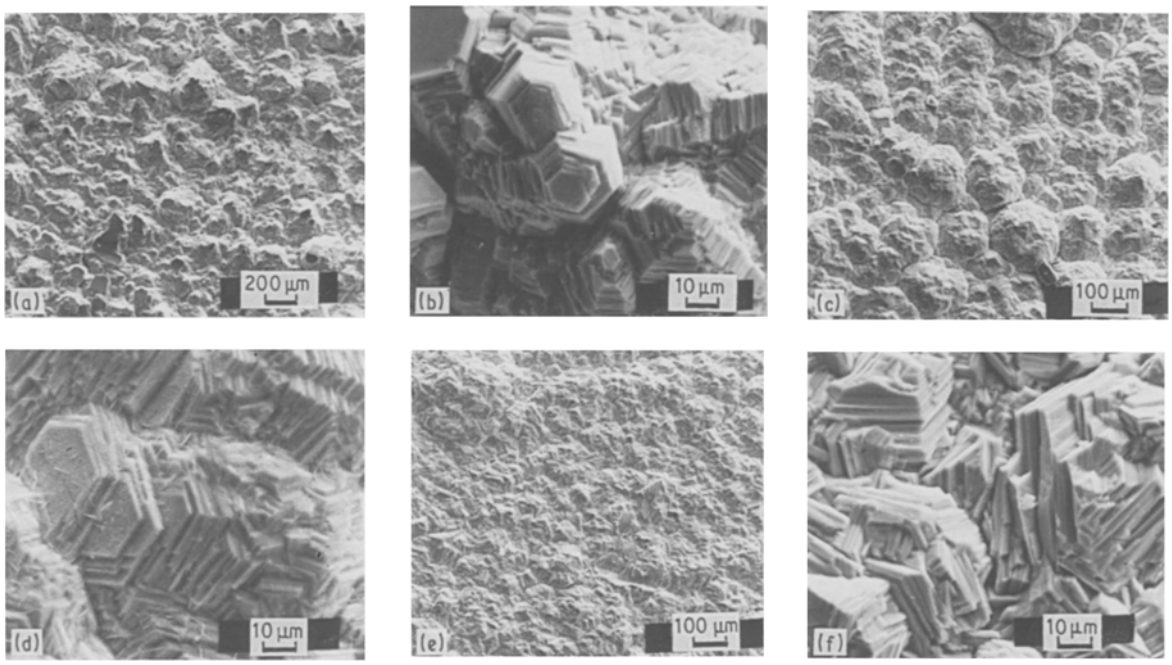

Fig. 2. SE micrographs showing the morphology of 6 h zinc deposits electrowon at 500 A m^{-2} and 38° C from electrolytes containing: (a) and (b) 0, (c) and (d) 30, and (e) and (f) 45 mg l^{-1} of glue.

cate that there is a gradual proportional increase in NOP with glue addition. After 6 h of electrolysis, however, the NOP remains essentially constant regardless of the glue concentration, Fig. 4.

3.2. *Antimony effect*

The effect of antimony additions (0–0.08 mg l^{-1}) on the CE for 6 h zinc deposits electrowon at 500 A m^{-2} and 38° C is summarized in Table 3 and a plot of CE against antimony concentration is presented in Fig. 5. For Sb > 0.02 mg l^{-1}, there is a significant decrease in CE; for Sb > 0.06 mg l^{-1}, the decrease in CE becomes disastrous and at 0.08 mg l^{-1} Sb, the CE is only 29.0%, Table 4.

The addition of 0.005 mg l^{-1} Sb to the electrolyte changed the deposit orientation from ⟨002⟩, ⟨103⟩ to ⟨114⟩, ⟨112⟩, ⟨103⟩, ⟨102⟩, ⟨101⟩ which persisted for Sb concentrations up to 0.02 mg l^{-1}, Table 3. This is reflected in the deposit morphology, Fig. 6b, which shows sharply defined hexagonal zinc platelets aligned at intermediate angles to the Al cathode. The low magnification SE micrograph, Fig. 6a, however, shows that at 0.02 mg l^{-1} Sb, the deposit surface consists of numerous circular depressions.

At 0.04 mg l^{-1} Sb, the circular depressions are more developed and appear as large circular holes in the surface, suggesting resolution of the deposit, Fig. 6c. The hexagonal zinc platelets are now aligned at low angles (< 30°) to the Al cathode, Fig. 6d, and this results in a ⟨105⟩, ⟨103⟩, ⟨114⟩ deposit orientation, Table 3. This trend persists for Sb = 0.06 mg l^{-1} as reflected in the low CE, 77.9% and the ⟨105⟩, ⟨103⟩, ⟨114⟩, ⟨102⟩, ⟨112⟩ preferred orientation, Table 3. At 0.08 mg l^{-1} Sb, the entire center of the deposit redissolved (see Fig. 9).

Table 3. The effect of antimony on the current efficiency, orientation and nucleation overpotential (NOP) for 6 h zinc deposits electrowon at 500 A m^{-2} and 38° C

Sb (*mg l^{-1}*)	*CE* (*%*)	*Orientation**	*NOP (mV against MSE)*	
			Initial	*Final*
0	91.0	002, 103	140	125
0.005	90.8	114, 112, 103, 102, 101	105	150
0.010	88.7	114, 103, 112, 102, 101	70	125
0.015	90.4	—	105	120
0.015	93.3	101, 201	85	135
0.020	86.7	103, 114, 112, 102, 101	65	120
0.020	90.8	114, 112, 103, 102, 101	60	90
0.025	85.3	114, 103, 112, 102, 101	65	120
0.040	85.6	105, 103, 114	50	92
0.060	77.9	105, 103, 114, 102, 112	60	87
0.080	29.0	—	55	85

* Relative to ASTM Standard for zinc powder.

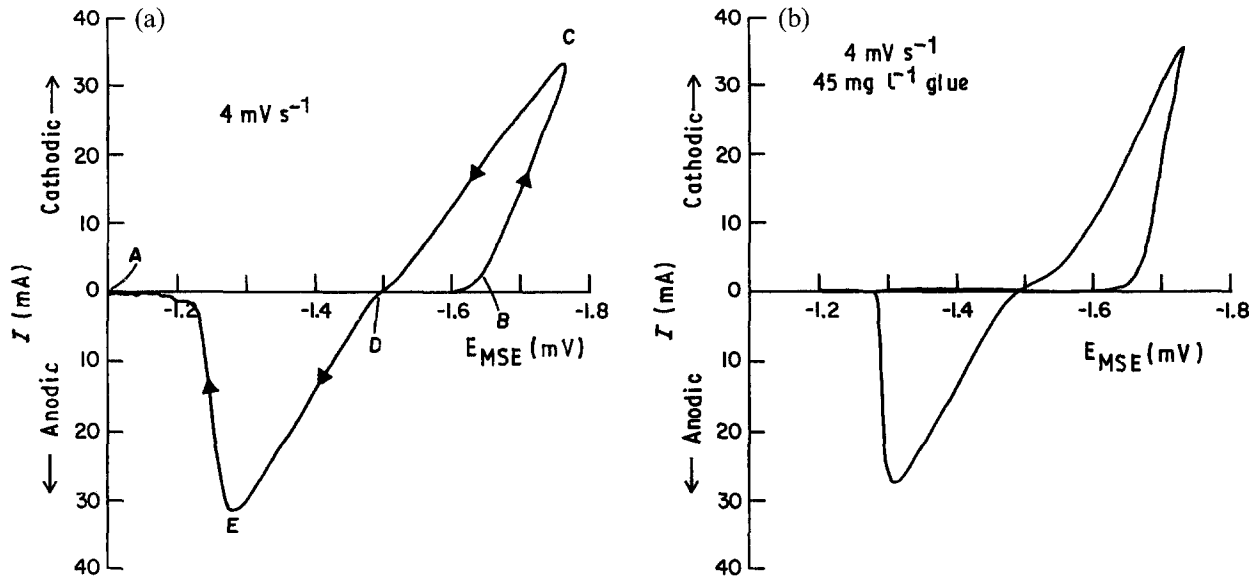

Fig. 3. Typical cyclic voltammograms for Kidd Creek zinc electrolyte containing: (a) 0 and (b) 45 mg l^{-1} glue.

A typical CV for Sb-containing electrolyte is shown in Fig. 7. As indicated, there is a significant decrease in the NOP for zinc deposition, and this reflects the strong depolarizing effect of Sb. The NOP values obtained for both the initial and final cell electrolytes as a function of Sb concentration are listed in Table 3. Between 0 and 0.02 mg l^{-1} Sb there is a large decrease in NOP, but thereafter, it remains fairly constant. The NOP values obtained in the presence of Sb in the initial cell electrolyte are significantly less than those for the final cell electrolyte; that is the reverse of the trend observed for the glue systems, Fig. 4. The average NOP values were 72 mV with respect to MSE for the initial electrolyte and 97 for the final cell electrolyte.

3.3. *Antimony + glue effects*

The effect of various antimony + glue combinations on the CE for 6 h zinc deposits electrowon at 500 A m^{-2} and 38° C is summarized in Table 4 and is shown in Fig. 8 as a series of plots of CE against glue concentration for each level of Sb. As the data indicate, for each Sb concentration there is an optimum glue value at which the CE is a maximum. A similar trend was reported by Robinson and O'Keefe [1] in their study of antimony-glue effects in Cominco electrolyte. In the present study it was observed that at 0.02 mg l^{-1} Sb, the CE reached a maximum of 92.4% with the addition of 5 mg l^{-1} glue, Fig. 8 and Table 4. This CE is greater than the average value of 91% obtained for the addition-free electrolyte. In fact, at 0.02 mg l^{-1} Sb, the CE remains >91% for all glue concentrations up to 60 mg l^{-1}.

The preferred deposit orientations obtained for all antimony-glue combinations for which the CE was a maximum are presented in Table 5. In each case the preferred orientation was ⟨114⟩, ⟨112⟩, ⟨103⟩, ⟨102⟩, ⟨101⟩. This preferred orientation also persisted for other antimony-glue combinations close to the optimum values. Variations from the preferred orientation occurred only when one additive was present in excess; for example, at high glue–low antimony, the preferred orientation was more glue-like; i.e. ⟨112⟩, ⟨101⟩. At low glue–high antimony, the preferred orientation became more basal; i.e. ⟨103⟩, ⟨002⟩.

The deposits obtained for some of the antimony + glue combinations are shown in Fig. 9. At 0 mg l^{-1} Sb, the deposit surface becomes smoother as the glue concentration in the electrolyte is increased; however,

Table 4. The effect of various antimony–glue combinations on the current efficiency of 6 h zinc deposits electrowon at 500 A m^2 and 38° C

	Current efficiency (%)				
Sb (mg l^{-1})	*0*	*0.02*	*0.04*	*0.06*	*0.08*
Glue (mg l^{-1})					
0	91.0	90.8	85.6	77.9	29.0
5	90.1	92.4	85.5	80.7	68.4
10	88.8	92.4	86.9	85.6	75.7
15	89.2	92.0	88.7	86.8	81.4
20	89.4	92.2	92.1	87.7	–
30	86.8	92.0	90.2	88.8	85.8
40	–	–	91.3	88.1	85.4
45	87.8	92.4	91.0	91.0	90.5
60	85.9	91.9	90.6	87.5	91.3

Table 5. Zinc deposit preferred orientation at optimum antimony–glue levels for 6 h zinc deposits electrowon at 500 A m^{-2} and 38° C

Sb (mg l^{-1})	*Glue (mg l^{-1})*	*Orientation*
0.02	5	114, 112, 103, 102, 101
0.04	20	114, 112, 103, 102, 101
0.06	45	114, 112, 103, 102, 101
0.08	60	114, 112, 103, 102, 101

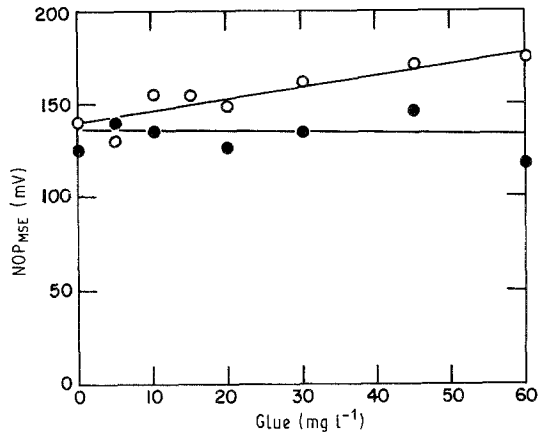

Fig. 4. Plots of nucleation overpotentials against glue concentration for initial (○) and final (●) cell electrolytes.

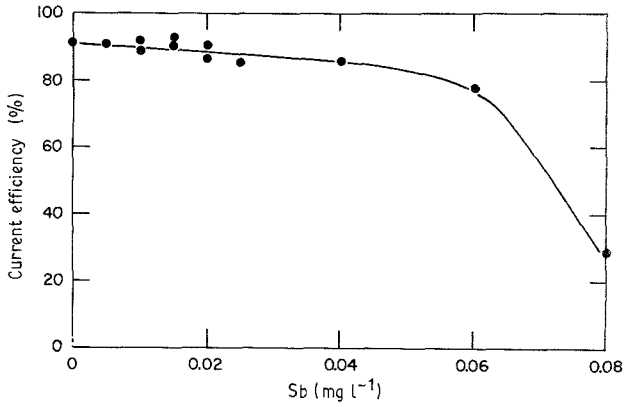

Fig. 5. Plot of current efficiency against antimony concentration for 6 h zinc deposits electrowon at 500 A m^{-2} and 38° C.

at 60 mg l^{-1} glue, fine crystalline nodules form on an initially smooth surface. At 0.04 mg l^{-1} Sb, the light circular area at the centre of the deposit indicates zinc re-solution; increasing the Sb concentration to 0.08 mg l^{-1} results in the re-solution of the entire centre of the zinc deposit. At 60 mg l^{-1} glue, the addition of 0.04 mg l^{-1} Sb removed the secondary growth from the surface of the deposit and increased the CE; at 0.08 mg l^{-1} Sb, the deposit surface was very smooth and the CE was a maximum, Table 4.

The deposit morphology obained at optimum antimony + glue additions; i.e. associated with the ⟨114⟩, ⟨112⟩, ⟨103⟩, ⟨102⟩, ⟨101⟩ preferred orientation, is shown in the SE micrographs in Fig. 10. The deposit surface consists of even rows of uniform, closely packed nodules, Fig. 10a, which in turn consists of sharply defined hexagonal zinc platelets aligned at intermediate angles to the Al cathode, Fig. 10b.

A typical cyclic voltammogram for antimony + glue-containing electrolytes is shown in Fig. 11. The

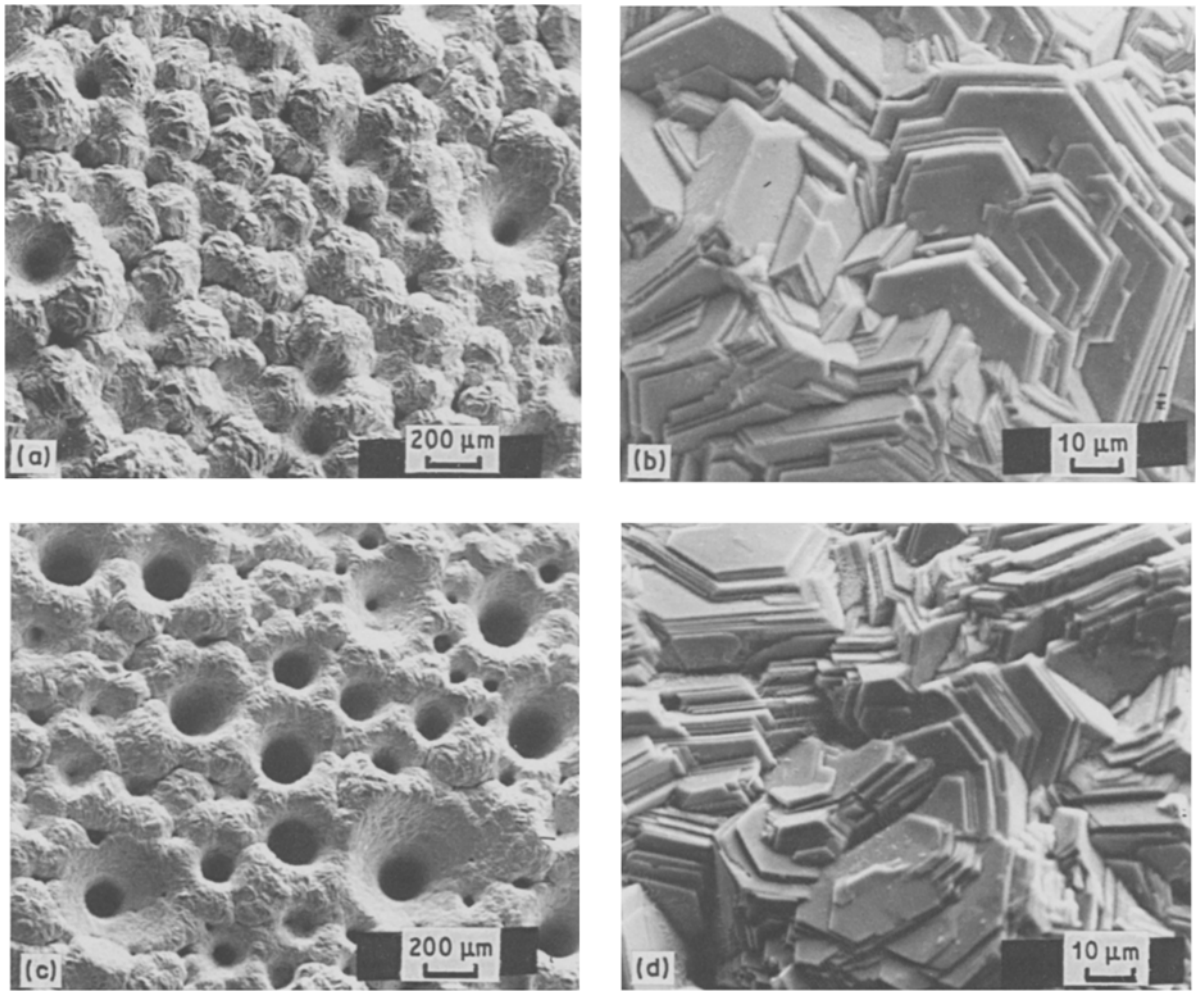

Fig. 6. SE micrographs showing the morphology of 6 h zinc deposits electrowon at 500 A m^{-2} and 38° C from electrolytes containing (a) and (b) 0.02 and (c) and (d) 0.04 mg l^{-1} Sb.

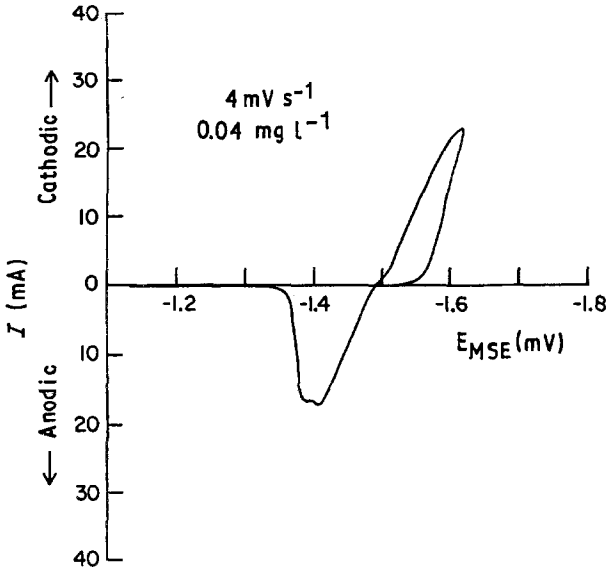

Fig. 7. Cyclic voltammogram for Kidd Creek zinc electrolyte containing 0.04 mg l^{-1} Sb.

NOP values obtained for the initial and final cell electrolytes containing various antimony + glue combinations are summarized in Table 6. Both the initial and final NOP values obtained for the various antimony–glue combinations were always less than those obtained for glue alone, thus indicating the depolarizing effect of antimony. At a fixed antimony concentration, both the initial and final NOP values increase with increasing glue concentration, Fig. 12 and Table 6. For glue concentrations > 10 mg l^{-1}, the final NOP value is always significantly less than the initial NOP value, Fig. 12.

The CE values obtained for all antimony–glue combinations were plotted against the corresponding initial and final NOP values and the results are presented in Figs 13 and 14. Although there is some scatter in the data points, these plots indicate that a maximum CE occurs at 120–130 mV with respect to MSE for the initial electrolyte and at 100–110 mV with respect to MSE for the final electrolyte. A similar CE–NOP correlation was observed for antimony-glue additions to Cominco electrolyte [13].

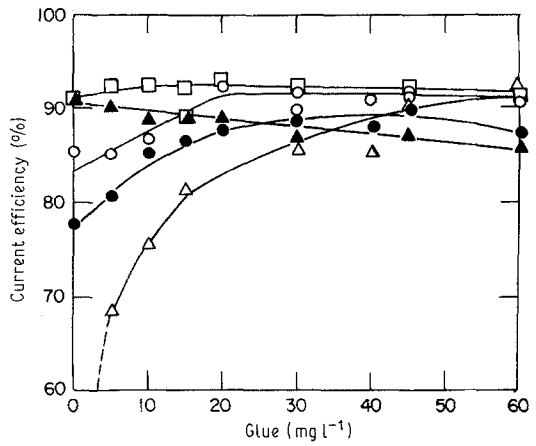

Fig. 8. Plots of current efficiency against glue concentration at various fixed antimony levels for 6 h zinc deposits electrowon at 500 A m^{-2} and 38° C: ▲ 0, □ 0.02, ○ 0.04, ● 0.06 and △ 0.08 mg l^{-1}.

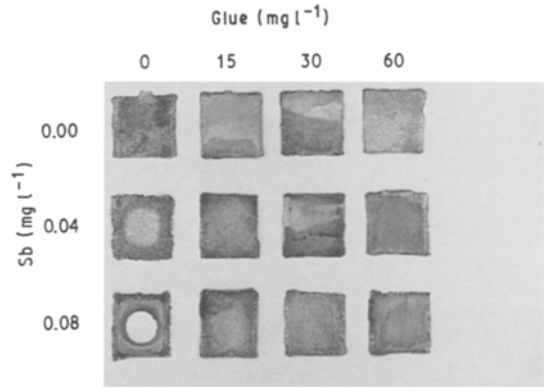

Fig. 9. Photograph showing the surface of 6 h zinc deposits electrowon at 500 A m^{-2} and 38° C from electrolytes containing various antimony–glue combinations.

4. Conclusions

Both the individual and combined effects of glue and antimony on zinc deposition current efficiency and polarization and on the morphology and orientation of 6 h deposits electrowon at 500 A m^{-2} and 38° C from Kidd Creek electrolyte were determined. Both

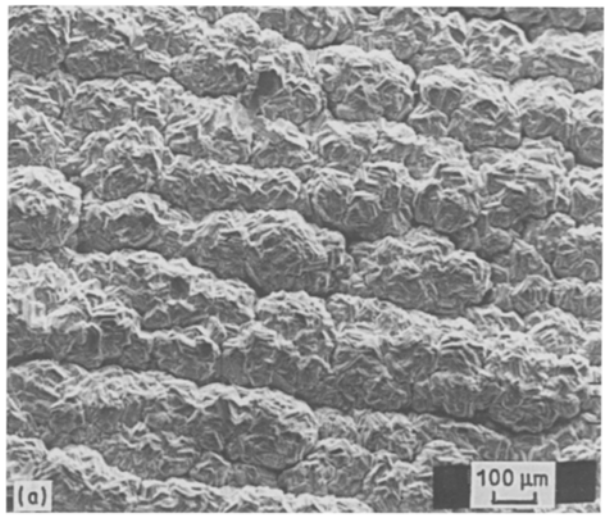

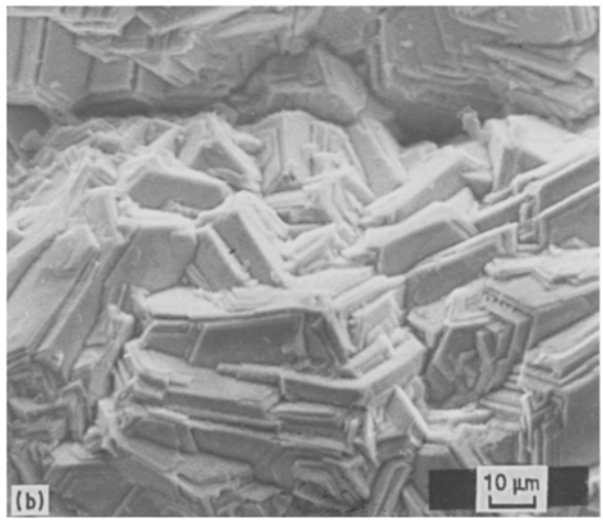

Fig. 10. SE micrographs showing the morphology of the 6 h zinc deposit electrowon at 500 A m^{-2} and 38° C from electrolyte containing optimum antimony–glue concentrations.

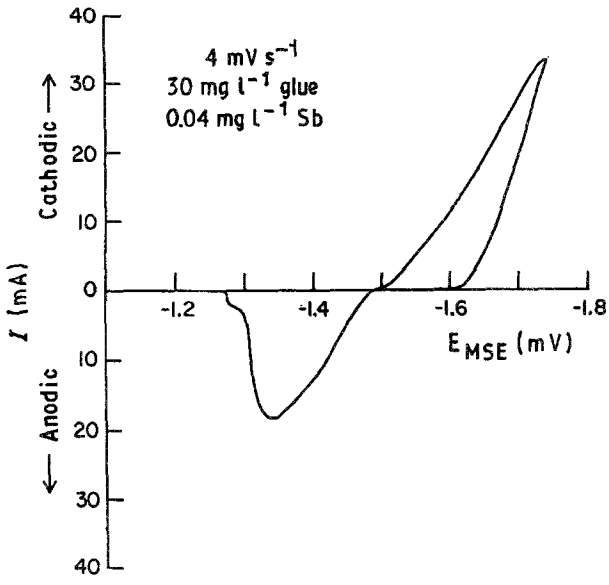

Fig. 11. Cyclic voltammogram for Kidd Creek zinc electrolyte containing optimum antimony–glue concentrations.

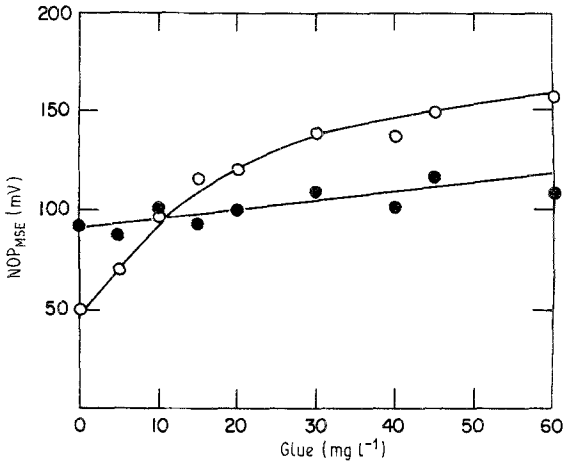

Fig. 12. Plots of nucleation overpotentials against glue concentration for initial (○) and final (●) cell electrolytes containing 0.04 mg l^{-1} antimony.

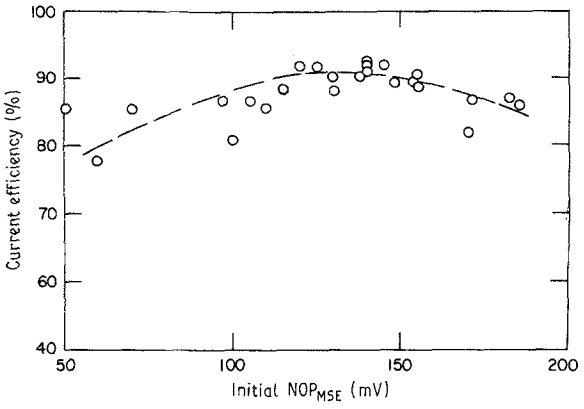

Fig. 13. Plot of current efficiency against initial nucleation overpotential obtained for electrolytes containing various concentrations of antimony and glue.

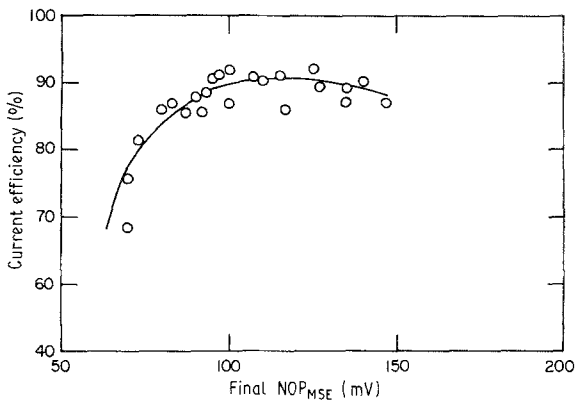

Fig. 14. Plot of current efficiency against final nucleation overpotential obtained for electrolytes containing various concentrations of antimony and glue.

glue and antimony decreased zinc deposition CE, and Sb was the more detrimental. Glue increased zinc deposition polarization, refined the deposit grain size and changed the preferred deposit orientation from ⟨002⟩, ⟨103⟩ to ⟨112⟩, ⟨101⟩, ⟨114⟩; in other words, from basal to intermediate. Antimony, at < 0.02 mg l^{-1}, changed the deposit orientation to ⟨114⟩, ⟨112⟩, ⟨103⟩, ⟨102⟩, ⟨101⟩; at higher concentrations Sb was a strong depolarizer and changed the preferred deposit orientation to ⟨105⟩, ⟨103⟩, ⟨114⟩; that is, basal. At a Sb concentration of 0.08 mg l^{-1}, severe re-solution of the 6 h zinc deposit occurred.

Certain combinations of antimony + glue were found to optimize the CE and consistently gave a ⟨114⟩, ⟨112⟩, ⟨103⟩, ⟨102⟩, ⟨101⟩ preferred deposit orientation. A correlation was also observed between the CE and NOP for zinc deposition such that the CE was a maximum when the NOP of the initial cell electrolyte was 120–130 mV with respect to MSE or when the NOP of the final cell electrolyte was 100–110 mV with respect to MSE.

Acknowledgements

Thanks are due to P. Carriere, CANMET, for undertaking the X-ray diffraction analyses, to T. T. Chen,

Table 6. The effect of antimony + glue on the initial and final nucleation overpotentials (NOP)

	Initial/Final nucleation overpotentials (mV against MSE)				
Sb (mg l^{-1})	*0*	*0.02*	*0.04*	*0.06*	*0.08*
Glue (mg l^{-1})					
0	140/125	60/90	50/92	60/87	55/85
5	130/140	80/83	70/87	100/87	70/70
10	155/140	105/90	97/100	110/77	80/70
15	155/135	105/90	115/112	105/77	105/83
20	150/133	130/90	120/100	130/90	–
30	161/135	125/95	130/100	124/89	125/90
40	–	–	137/100	135/87	135/85
45	170/147	140/95	150/115	140/87	137/95
60	175/117	145/100	155/107	163/100	147/97

CANMET, for the SEM photographs and to Kidd Creek for supplying electrolyte, addition reagents and electrode materials, and for permission to publish this work.

References

[1] D. J. Robinson and T. J. O'Keefe, *J. Appl. Electrochem.* **6** (1976) 1.
[2] D. J. MacKinnon, J. M. Brannen and P. L. Fenn, *ibid.* **17** (1987) 1129.
[3] D. J. MacKinnon and J. M. Brannen, *ibid.* **7** (1977) 451.
[4] D. R. Fosnacht and T. J. O'Keefe, *ibid.* **10** (1980) 495.
[5] D. R. Fosnacht and T. J. O'Keefe, *Met. Trans.* **14B** (1983) 645.
[6] P. A. Adcock, A. R. Ault and O. M. G. Newman, *J. Appl. Electrochem.* **15** (1985) 865.
[7] F. Laist, R. B. Caples and G. T. Wever, in Handbook of Nonferrous Metallurgy, Recovery of Metals (edited by D. M. Liddell), McGraw Hill, New York (1945) p. 379.
[8] F. S. Weirner, G. T. Wever and R. J. Leper, in 'Zinc, The Science and Technology of the Metal, its Alloys and Compounds' (edited by C. H. Mathewson), ACS Monograph Series, Reinhold, New York (1959) p. 174.
[9] C. T. Wever, *J. Metals* **11** (1959) 130.
[10] C. L. Mantell, 'Electrochemical Engineering' (4th edn), McGraw Hill, New York (1960) p. 210.
[11] A. R. Ault and E. J. Frazer, *J. Appl. Electrochem.* **18** (1988) 583.
[12] B. A. Lamping and T. J. O'Keefe, *Met. Trans.* **7B** (1976) 551.
[13] R. C. Kerby and C. J. Krauss, Continuous Monitoring of Zinc Electrolyte Quality at Cominco by Cathodic Overpotential Measurements, in 'Lead–Zinc–Tin '80' (edited by J. M. Cigan, T. S. Mackey and T. J. O'Keefe), TMS-AIME, New York (1979) 187.
[14] D. J. MacKinnon, J. M. Brannen and R. C. Kerby, *J. Appl. Electrochem.* **9** (1979) 71.
[15] E. Rolia and J. E. Dutrizac, *Can. Metall. Quart.* **23** (1984) 159.